JACS
JOURNAL OF THE AMERICAN CHEMICAL SOCIETY
Article
pubs.acs.org/JACS

Lower the Electron Affinity by Halogenation: An Unusual Strategy To Design Superalkali Cations

Na Hou, Di Wu, Ying Li,* and Zhi-Ru Li

Institute of Theoretical Chemistry, State Key Laboratory of Theoretical and Computational Chemistry, Jilin University, Changchun 130023, P. R. China

Supporting Information

ABSTRACT: A new kind of cationic superatom compounds $(M-F)^+$ ($M = OLi_4$, NLi_5, CLi_6, BLi_7, and Al_{14}) with low vertical electron affinities (VEA) has been designed based on the distinctive electronic structure of superalkaline-earth atom. The stability of the studied superatom architectures is guaranteed by strong M−fluorine interactions, considerable HOMO−LUMO gaps, as well as large dissociation energies. What is extraordinary is that fluorination plays an important role in lowering the VEA value of M^+ and enables the resulting $(M-F)^+$ fluorides to join the superalkali family. However, the same strategy does not work as well for the alkaline-earth atoms whose valence electrons are more tightly bound. The comparative study on $(OLi_4-X)^+$ (X = F, Cl, Br) reveals that fluorination is more effective than chlorination and bromination to reduce the VEA value of the OLi_4^+ cation. As for the $(Al_{14}-X)^+$ species, there is no obvious dependence of VEA values on halogen atomic number.

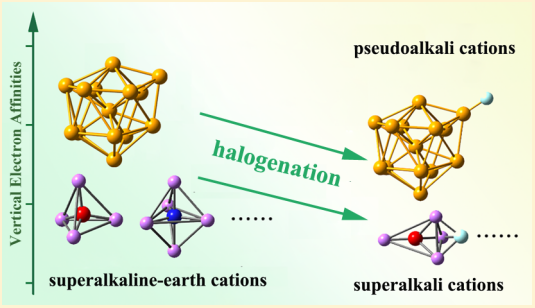

1. INTRODUCTION

In preliminary work, Khanna and Jena have proposed that atomic clusters with suitable size and composition could mimic the chemical behavior of atoms in the periodic table. Such intriguing species are, hence, termed as "superatoms"[1,2] and have attracted extensive attention. Two dominant subsets of superatoms are superhalogens and superalkalis which were initially introduced in chemistry by Gutsev and Boldyrev.[3,4] Superhalogens are molecules possessing very large electron affinities, exceeding the 3.617 eV (Cl)[5] atomic electron affinity (EA) limit. Because of this, superhalogens almost always exist as negative ions, usually as the anionic portions of salts.[6] As previously stated, most superhalogen anions match the $(M_nX_{nk+1})^-$ formula (where M is an electropositive atom, k is the maximal formal valence of M, and X corresponds to any ligand with high EA). The halogens are often used as ligands in superhalogens as they are known to have the highest EA among all the chemical elements. The concept of superalkali is used to describe polyatomic systems whose ionization potentials (IPs) are lower than that (3.89 eV)[7] of cesium atom. Most superalkalis coincide with the formula ML_{k+n} (where M represents an electronegative atom or functional group and L is an alkali metal atom). Accordingly, their daughter cations possess very low EAs. During the past 30 years, there has been increasing interest and activity in both experimental[8−13] and theoretical[14−20] investigations of these two classes of superatoms. As a consequence, some molecules with extremely high EAs or considerably low IPs were experimentally confirmed. Recently, our group has focused on superalkali design and reported a series of binuclear[21,22] and polynuclear superalkali cations[23,24] with considerably lower vertical electron affinities (VEAs). Furthermore, we have proposed unusual superalkali cations using hydrogen as ligands, namely $M_2H_{2n+1}^+$ (M = F, O, N, C), thereby introducing nonmetallic members into this research area.[25]

Meanwhile, the attempts to identify other superatom motifs have yielded exciting results. It is known that the valence of Al can be 1 or 3 in small clusters.[26,27] Likewise, it has been found that the Al_7^- cluster exhibits valence of 2 and 4, which makes it analogous to C or Si and be classified as a multiple valence superatom.[28] An Al_{14} cluster behaves like an alkaline earth atom when combined with iodine atoms to form the $Al_{14}I_x^-$ cluster compounds and hence can be regarded as a superalkaline earth atom.[29] In 2003, the concept of magnetic superatom was introduced by Kumar et al.[30] Afterward, Khanna and co-workers have proposed a theoretical approach to design magnetic superatoms such as VCs_8,[31] VNa_8,[31] $TiNa_9$,[32] and $FeMg_8$,[33] etc. Recently, they have presented experimental evidence of the existence of VNa_8, which opens the pathway to investigate the spin-dependent electronics of the new magnetic motifs.[34]

Recent developments in the field of superatom chemistry also brought forward various compounds, clusters, and extended assemblies with superatoms as the building blocks. A known example is the superatom compound formed by combining the Al_{13} cluster with superalkalis (K_3O and Na_3O). The resulting $Al_{13}M_3O$ (M = Na, K) motifs are strongly bound

Received: November 18, 2013
Published: January 31, 2014

   dx.doi.org/10.1021/ja411755t | J. Am. Chem. Soc. 2014, 136, 2921−2927

molecules and can be assembled into stable superatom assemblies $(Al_{13}M_3O)_n$.[35] Afterward, Wu and co-workers presented the theoretical evidence for a series of superatom compounds, including Li_3−SH (SH = LiF_2, BeF_3, and BF_4),[36] BLi_6−X (X = F, LiF_2, BeF_3, and BF_4),[37] and BF_4−M (M = Li, FLi_2, OLi_3, and NLi_4).[38] Herein, BLi_6−X and BF_4−M may represent potential nonlinear optical (NLO) molecules because of their large bond energies and considerable NLO responses. In addition, a type of endohedral metallofullerene−superhalogen compounds Li@C_{60}−BX_4 (X = F, Cl, Br) has been theoretically characterized. It is found that the first hyperpolarizability of Li@C_{60} can be enhanced by introducing proper superhalogens.[39] By investigating the geometric, electronic, and optical properties of the superatomic heterodimer Sc@Si_{16}−V@Si_{16} and trimer Sc@Si_{16}−Ti@Si_{16}−V@Si_{16}, Iwasa and Nakajima[40] have indicated that the close-packed assembly of the superatomic monomers M@Si_{16} (M = Sc, Ti, V) might open new avenues in nanocluster-assembled device engineering for electronics and optics. Undoubtedly, these achievements have reinforced the idea that the potential of creating new superatoms or superatom architectures with desirable properties is limitless.

In this work, we have designed a series of superalkaline-earth-based cationic compounds $(M-F)^+$ (M = OLi_4, NLi_5, CLi_6, BLi_7, and Al_{14}) and investigated their structures and properties by means of ab initio methods and density functional theory. Herein, the Al_{14} and BLi_7 clusters exhibit superalkaline earth nature, which has been proposed in previous works.[29,41] The OLi_4,[42] NLi_5, and CLi_6[43] clusters with a $1s^21p^62s^2$ electronic configuration can also be viewed as superalkaline earth atoms. The strong interaction between superatom M and fluorine, as well as the large dissociation energies of the $(M-F)^+$ cations, guarantees the stability of these superatom architectures. Interestingly, fluorination has been found to lower the electron affinity of M^+, which is attributed to the electronic structure features of the superalkaline-earth metal atom. Consequently, the studied fluorides exhibit low vertical electron affinities (VEAs), and the VEA values (3.42−3.85 eV) of the $(M-F)^+$ (M = OLi_4, NLi_5, CLi_6, and BLi_7) cations are even lower than the IP = 3.89 eV of the Cs atom. In addition, the $(OLi_4-X)^+$ and $(Al_{14}-X)^+$ (X = Cl, Br) compounds are investigated in parallel to determine whether their VEA values are halogen atomic number related.

2. COMPUTATIONAL DETAILS

First, we considered different interaction orientations between F and superalkaline earth M and brought F toward M along an on-top, bridge, or hollow site above the M polyhedron, and the resulting geometry was fully optimized without any symmetry constraints. In order to ensure the lowest energy structure of $(M-F)^+$, the randomized algorithm[44] was also used to search for all possible isomers of $(OLi_4-F)^+$, $(NLi_5-F)^+$, $(CLi_6-F)^+$, and $(BLi_7-F)^+$. It is found that the global minimum structures obtained by means of manual and random approaches are consistent. Structures of the $(M-F)^+$ (where M = OLi_4, NLi_5, CLi_6, and BLi_7) species were optimized by employing the MP2 method, while the geometry of the larger $(Al_{14}-F)^+$ compound was optimized using the B3LYP[45] method. In the geometry optimization and the following calculations, the 6-311+G(3df) basis set was adopted for the $(M-F)^+$ (M = OLi_4, NLi_5, CLi_6, and BLi_7) systems, and the smaller 6-311+G(d) basis set was used for $(Al_{14}-F)^+$. Vibrational frequencies and natural bond orbital (NBO)[46,47] analyses were carried out at the same level as the geometry optimization. The vertical electron affinities (VEA) of the $(M-F)^+$ cations, defined as the total energy difference between the neutral and cationic systems at the cation geometry, were calculated on the basis of the restricted outer valence Green function (OVGF)[48−50] method. The bond energies (E_b) between the M and F subunits of the $(M-F)^+$ (M = OLi_4, NLi_5, CLi_6, and BLi_7) compounds were obtained at the CCSD(T)/6-311+G(3df) level. For $(Al_{14}-F)^+$, the E_b values were calculated at the MP2/6-311+G(d) level. We used the counterpoise (CP)[51] procedure to eliminate the basis set superposition error (BSSE) effect given by eq 1[52]

$$E_b = E_A(X_{AB}) + E_B(X_{AB}) - E_{AB}(X_{AB}) \quad (1)$$

where the same basis set, X_{AB}, was used for the subunit energy (E_A and E_B) calculation as for the compound energy (E_{AB}) calculation.

All calculations were performed using the GAUSSIAN 09 program package.[53] The plots of molecular configurations and orbitals were generated with the GaussView program.[54]

3. RESULTS AND DISCUSSION

3.1. Structures and Stability of the $(M-F)^+$ (M = OLi_4, NLi_5, CLi_6, and BLi_7) Species. The optimized structures of the superalkaline-earth fluoride cations $(M-F)^+$ (M = OLi_4, NLi_5, CLi_6, and BLi_7) are shown in Figure 1, and the symmetry

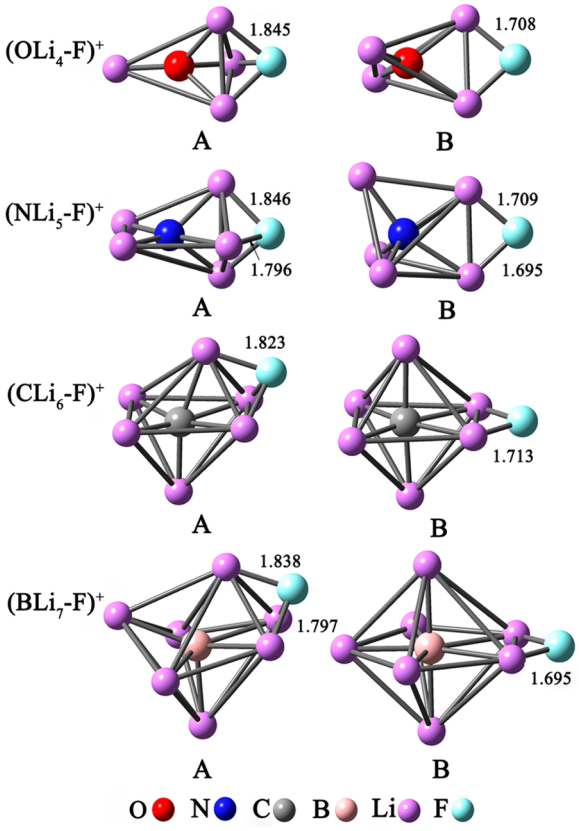

Figure 1. Optimized structures of the $(M-F)^+$ (M = OLi_4, NLi_5, CLi_6, and BLi_7) cations at the MP2/6-311+G(3df) level. The F−Li bond lengths are in angstroms.

group, bond energies, and NBO charges on F atoms of the $(M-F)^+$ series are presented in Table 1. From Figure 1, two isomers (**A** and **B**) were obtained for each $(M-F)^+$ cation. Specifically, the fluorine atom may occupy the hollow or the bridge site of the M polyhedron, and the former location of F generates the lowest energy structure **A**. This is the same case for the interaction between polyhedral superalkali BLi_6 and F atom.[37] Note that the F−Li bonds in structure **A** are longer by 0.087−0.151 Å than those in isomer **B** because the F atom interacts with more Li atoms in **A**.

dx.doi.org/10.1021/ja411755t | J. Am. Chem. Soc. 2014, 136, 2921−2927

Table 1. Symmetry Point Group, Relative Energies, E_{rel} (in kcal/mol), HOMO−LUMO Gaps (in eV), Bond Energies, E_b (in kcal/mol), Vertical Electron Affinities, VEA (in eV), and NBO Charges on F atoms (q^F) of the $(M-F)^+$ (M = OLi_4, NLi_5, CLi_6, and BLi_7) Cations

species	isomer	symmetry	E_{rel}	gap	E_b	VEA	q^F
$(OLi_4-F)^+$	**A**	C_{3v}	0.00	11.44	168.8	3.42	−0.856
	B	C_{2v}	3.70	11.46	160.6	3.79	−0.863
$(NLi_5-F)^+$	**A**	C_s	0.00	7.70	166.7	3.57	−0.839
	B	C_s	3.77	8.34	156.9	3.85	−0.850
$(CLi_6-F)^+$	**A**	C_{3v}	0.00	6.62	165.7	3.64	−0.834
	B	C_{2v}	8.85	6.65	153.1	3.83	−0.846
$(BLi_7-F)^+$	**A**	C_s	0.00	5.52	167.6	3.69	−0.846
	B	C_{2v}	4.64	5.79	158.1	3.84	−0.856
OLi_4^+						4.37[a]	
NLi_5^+						4.30[a]	
CLi_6^+						4.25[a]	
BLi_7^+						4.20[a]	

[a]Computed at the B3LYP//B3LYP/6-311+G(3df) level.

For comparison, the structures of OLi_4, NLi_5, CLi_6, and BLi_7 are optimized at the MP2/6-311+G(3df) level and displayed in the Supporting Information, Figure S1. From Figure 1 and Figure S1 (Supporting Information), it is discerned that the structural integrity of these superalkaline earth metals is basically maintained after fluorination.

The HOMO−LUMO energy gap is a useful quantity for examining the stability of clusters. From Table 1, the HOMO−LUMO gaps of the $(M-F)^+$ (M = OLi_4, NLi_5, CLi_6, and BLi_7) compounds range from 5.52 to 11.46 eV. These gap values are comparable to those of 7.58−10.58 eV for stable superalkali cations OM_3^+ (M = Li, Na, K),[55] indicating the high stability of the investigated cations.

As shown in Table 1, the $(M-F)^+$ (M = OLi_4, NLi_5, CLi_6, and BLi_7) compounds possess large bond energies of 153.1−168.8 kcal/mol at the CCSD(T)/6-311+G(3df) level. Using the same method, the bond energy of the experimentally identified alkaline-earth fluoride cation MgF^+[56] is calculated to be 99.2 kcal/mol. By contrast, the E_b values of the $(M-F)^+$ cations are large enough to show the strong interaction between superalkaline earth M and fluorine. We note that the global minimum structure **A** contains one more Li−F connection than structure **B**. This is why the former exhibits larger bond energy than the latter by 8.2−12.6 kcal/mol.

The bonding nature between superatom M (OLi_4, NLi_5, CLi_6, and BLi_7) and F atom is explored on the basis of NBO and atom-in-molecule (AIM)[57] analyses. From Table 1, the NBO charge on F atom varies in the $-0.834|e| \sim -0.863|e|$ range, suggesting that an electron transfers from superalkaline-earth M to F. Hence, the M moiety exhibits a +2 valence state in the $(M-F)^+$ species that can consequently be written as $M^{2+}F^-$. This implies that a $(M-F)^+$ is an ionic-bound compound much like an MgF^+. On the other hand, the AIM theory can also help us to study the nature of interaction. The Laplacian of the electron density at a bond critical point, $\nabla^2\rho(r)$, can be used to describe the covalent bonds, ionic bonds, hydrogen bonds, and van der Waals interactions. We calculated the $\nabla^2\rho(r)$ values for all the Li−F bonds that connect M and F subunits at the MP2/6-311+G(3df) level. The results range from 0.274 to 0.464 au, also indicating that the superalkaline-earth atom M and fluorine are connected by ionic bonds.

To examine the thermodynamic stability of these superatom compounds, the dissociation energies of selected fragmentation pathways were calculated. We considered four possible dissociation channels for the $(M-F)^+$ species, namely, emission of F^-, FLi_2^+, Li^+, and LiF molecules, respectively (see Table S1, Supporting Information). The zero-point-corrected dissociation energies ΔE at the MP2/6-311+G(3df) level are collected in Table 2. Take the $(OLi_4-F)^+$ system as an example. ΔE_1, ΔE_2, ΔE_3, and ΔE_4 represent the reaction energies of the dissociation channels $(OLi_4-F)^+ \rightarrow OLi_4^{2+} + F^-$, $(OLi_4-F)^+ \rightarrow OLi_2 + FLi_2^+$, $(OLi_4-F)^+ \rightarrow OLi_3F + Li^+$ and $(OLi_4-F)^+ \rightarrow OLi_3^+ + LiF$, respectively. From Table 2, we can see that the preferred dissociation channel with the smallest reaction energy for an $(M-F)^+$ cation is the emission of a LiF molecule. Still, this reaction requires large reaction energies of 35.45−55.16 kcal/mol. Thus, the considered $(M-F)^+$ species are very stable against decomposition. The ΔE_1 values are much larger than the others, showing that the F^- anion is tightly bound to superalkaline-earth dication M^{2+}.

Table 2. Dissociation Energies ΔE (kcal/mol) of the $(M-F)^+$ Cations, Computed According to Four Dissociation Channels Shown in Table S1 (Supporting Information)

species	isomer	ΔE_1	ΔE_2	ΔE_3	ΔE_4
$(OLi_4-F)^+$	**A**	259.89	67.35	65.26	48.86
	B	256.43	63.94	61.80	45.37
$(NLi_5-F)^+$	**A**	252.51	65.26	64.11	41.29
	B	248.82	61.75	60.65	37.78
$(CLi_6-F)^+$	**A**	246.52	62.06	68.95	55.16
	B	238.21	53.65	60.65	46.75
$(BLi_7-F)^+$	**A**	244.44	53.65	55.58	39.91
	B	240.06	49.20	51.19	35.45

3.2. Structural and Bonding Features of the $(Al_{14}-F)^+$ Cation.

The global minimum (**A**) and 12 low-lying structures (**B**−**M**) of the $(Al_{14}-F)^+$ cation are shown in Figure 2. The symmetry, bond energies, and NBO charges on F atoms of the $(Al_{14}-F)^+$ cations are summarized in Table 3. From Figure 2, though the structural integrity of Al_{14} is not destroyed by fluorination, its geometry is distorted in some $(Al_{14}-F)^+$ isomers. Two types of bonding pattern for $(Al_{14}-F)^+$ can be noticed, one with the F atom occupying the on-top site (**A**, **B**, **G**) and the other with F at the bridge site of the Al_{14} moiety. Different from the case for the above-discussed $(M-F)^+$ (M = OLi_4, NLi_5, CLi_6, and BLi_7) species, no F face-capped structure

dx.doi.org/10.1021/ja411755t | J. Am. Chem. Soc. 2014, 136, 2921−2927

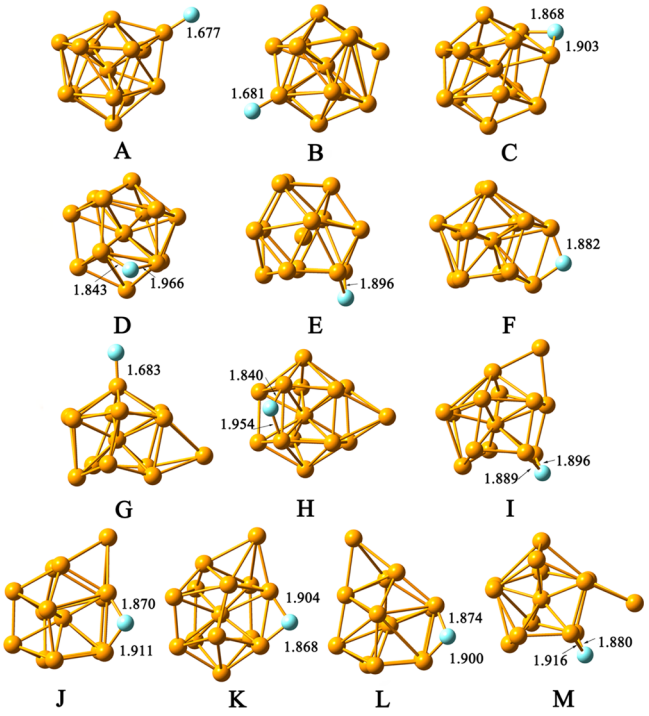

Figure 2. Optimized structures of the $(Al_{14}–F)^+$ cations at the B3LYP/6-311+G(d) level. The F–Al bond lengths are in angstroms.

Table 3. Symmetry Point Group, Relative Energies, E_{rel} (in kcal/mol), HOMO-LUMO Gaps (in eV), Bond Energies, E_b (in kcal/mol), Vertical Electron Affinities, VEA (in eV), and NBO Charges on F Atoms (q^F) of the $(Al_{14}–F)^+$ Cations

isomer	symmetry	E_{rel}	gap	E_b	VEA	q^F
A	C_{2v}	0.00	2.59	136.8	4.87	−0.747
B	C_s	0.19	2.58	136.8	4.81	−0.756
C	C_1	9.73	2.12	140.4	4.68	−0.792
D	C_s	10.98	2.36	137.2	4.81	−0.801
E	C_s	14.75	2.34	130.5	4.60	−0.781
F	C_{2v}	15.56	2.14	146.9	4.60	−0.808
G	C_1	27.23	1.89	125.4	4.95	−0.767
H	C_1	30.94	1.66	111.7	4.93	−0.768
I	C_1	31.25	1.68	124.6	4.77	−0.777
J	C_1	32.00	1.76	126.1	4.90	−0.781
K	C_1	32.94	1.73	120.5	5.06	−0.772
L	C_1	33.20	1.86	120.8	4.90	−0.775
M	C_1	35.77	1.95	120.4	4.66	−0.791
Al_{14}^+					5.22[a]	

[a]Computed at the B3LYP//B3LYP/6-311+G(d) level.

was found for $(Al_{14}–F)^+$. The Al–F bond lengths are 1.677, 1.681, and 1.683 Å for structures **A**, **B**, and **G**, respectively. In contrast, the other 10 structures have much longer Al–F bond lengths (1.840–1.966 Å) due to the formation of Al–F–Al bond.

The C_{2v}-symmetrical structure **A** is derived from a capped icosahedronal Al_{14} moiety, with F atom linking to the capping aluminum atom. Herein, the Al_{14} subunit is similar in geometry to the stable Al_{14}^{2+} dication.[58] The second isomer **B** is only 0.19 kcal/mol higher in energy than **A**. The Al_{14} moiety in **B** can also be viewed as a capped icosahedron. The same is valid for isomers **C** and **D**. From Figure 2, the F atom is located opposite the capping Al atom in structure **B**. Both **C** and **D** have side-on bound configurations, and their energy difference is only 1.25 kcal/mol. The geometry of the Al_{14} subunit in isomer **E** looks like a bottomless cage, and it is seen to lose its initial shape from isomer **E** onward. The Al_{14} moiety in isomer **F** resembles that in structure **B** with the bottom Al atom migrating to the top position. Meanwhile, **F** is 15.37 kcal/mol less stable than isomer **B**. The bottom Al atom in the Al_{14} part of isomer **A** caps an Al_4 quasi-quadrangle to generate the Al_{14} subunit in isomer **G**, while **G** is 27.23 kcal/mol less stable than **A**. The next isomer, **H**, is 3.71 kcal/mol higher in energy than **G**. The geometry of the Al_{14} subunit of isomer **H** is a tricapped pentagonal prism. The Al_{14} subunit of isomer **I** can be obtained from that of **G** by moving the capping Al atom to the top bridge position. Isomer **I** is found to be 4.02 kcal/mol less stable than **G**. Isomers **J** and **L** show great structural similarity, and the total energy difference between them is only 1.20 kcal/mol. As can be seen from Figure 2, the capping Al atom is located near the F atom in the former and located opposite the F atom in the latter. Isomer **K** adopts a distorted capped icosahedronal geometry of Al_{14}, with the F atom occupying a bridge site. **M**, the least favorable structure here, is 35.77 kcal/mol less stable than **A**. The geometry of **M** is similar to that of isomer **I**. The major difference between them is that the capping aluminum atom located adjacent to fluorine atom in **M**.

From Table 3, the HOMO–LUMO gaps of $(Al_{14}–F)^+$ are in the range of 1.66–2.59 eV, which are fairly large compared with that of 1.24 eV of the superatom compound $Al_{13}K_3O$.[35] Herein, the lowest energy structure **A** exhibits the largest gap value. Among the 13 isomers considered, the charges of Al_{14} subunit are within the range of 1.747|e| ∼ 1.808|e|, indicating that the Al_{14} cluster behaves like a divalent cation in the $(Al_{14}–F)^+$ cations. From Table 3, the NBO charge of F (−0.747|e| ∼ −0.808|e|) in each $(Al_{14}–F)^+$ system is close to −1. In addition, the $\nabla^2\rho(r)$ values of 0.257–0.947 au confirm the ionic bonding nature of all the Al–F bonds. Hence, the superatom compound $(Al_{14}–F)^+$ can also be characterized as ionic $(Al_{14}^{2+})F^-$. In addition, the $(Al_{14}–F)^+$ compounds possess large bond energies of 111.7–146.9 kcal/mol, which reflects a strong combination of Al_{14} and fluorine.

3.3. Halogenation Helps Lower Electron Affinities of M^+ (M = OLi_4, NLi_5, CLi_6, BLi_7, and Al_{14}). The vertical electron affinities (VEA) of the $(M–F)^+$ (M = OLi_4, NLi_5, CLi_6, and BLi_7) species are presented in Table 1, and those of the $(Al_{14}–F)^+$ isomers are listed in Table 3. The VEA values of the $(M–F)^+$ (M = OLi_4, NLi_5, CLi_6, and BLi_7) cations are as low as 3.42–3.85 eV, which are even lower than the IP = 3.89 eV of the Cs atom. Hence, the $(OLi_4–F)^+$, $(NLi_5–F)^+$, $(CLi_6–F)^+$, and $(BLi_7–F)^+$ species can be classified as superalkali cations and belong to the superalkali family. For comparison, the VEAs of the OLi_4^+, NLi_5^+, CLi_6^+, and BLi_7^+ cations were calculated to be 4.37, 4.30, 4.25, and 4.20 eV, respectively (see Table 1). Obviously, fluorination greatly lowers the vertical electron affinity of superalkaline-earth metal cation M^+. As for the $(Al_{14}–F)^+$ species, they may be regarded as pseudoalkali cations because their VEA values of 4.60–5.06 eV are above the 3.89 eV threshold but lower than the IP = 5.14 eV of the Na atom.[7] Though these VEA values are not low enough to ensure the superalkali identity of the $(Al_{14}–F)^+$ cations, they are still much lower than that of 5.22 eV for Al_{14}^+ (Table 3). Thus, a question emerges: now that the halogen atoms are known for their high electron affinities, how can fluorination, on the contrary, have a positive effect on decreasing the vertical electron affinity of a superalkaline-earth cation?

dx.doi.org/10.1021/ja411755t | J. Am. Chem. Soc. 2014, 136, 2921–2927

In order to reveal the answer to the above question, we start with the analysis of the electronic structure of the neutral M−F (M = OLi_4, NLi_5, CLi_6, and BLi_7) compounds. Take the lowest energy isomer **A** as an example. The optimized structures and the NBO charges on F atoms of the neutral M−F species at the B3LYP/6-311+G(3df) level are shown in Figure S2 (Supporting Information), and the vertical ionization potential (VIP) values of the M and M−F molecules at the same level are shown in Table S2 (Supporting Information). The singly occupied molecular orbitals (SOMOs) of the M^+ and M−F species are shown in Figure 3. From Figure S2, the F atom in

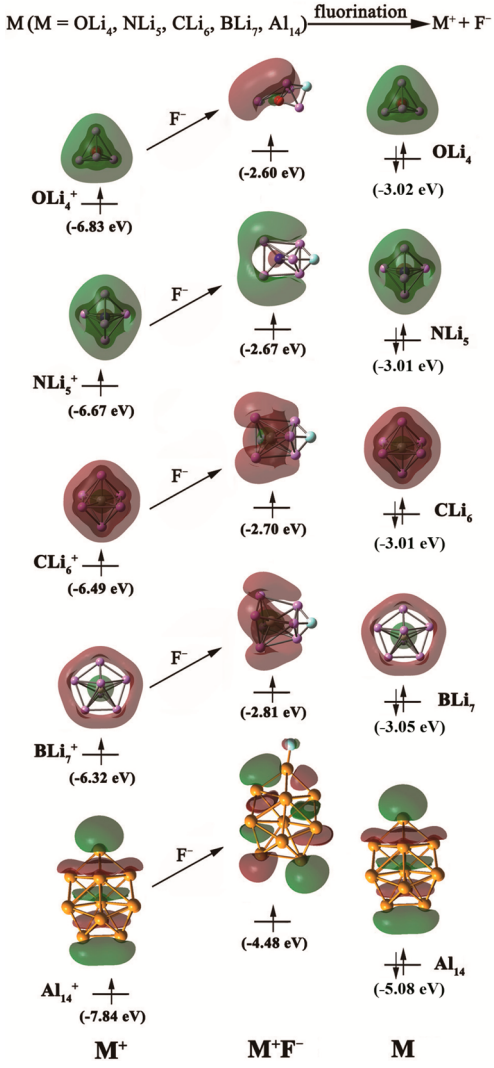

Figure 3. SOMOs of M^+ and M−F, HOMOs of M (M = OLi_4, NLi_5, CLi_6, BLi_7) molecules at the B3LYP/6-311+G(3df) level, and SOMOs of Al_{14}^+ and Al_{14}−F (isomer **A**), HOMO of Al_{14} at the B3LYP/6-311+G(d) level. The corresponding orbital energies are shown in parentheses.

the M−F molecules carries −0.846|e| ∼ −0.875|e| NBO charges, indicating an electron transfer from M to F. It is known that the electronic configuration of superalkaline earth metal M is $1s^21p^62s^2$, so the M^+ subunit of the resulting M^+F^- compound has one 2s electron left. As can be seen from the SOMOs of M^+F^-, the electron cloud is repulsed by the F^- anion and protrudes against fluorine, which leads to two effects. First, destroying the uniform distribution of the valence electron cloud and consequently destabilizing the SOMOs. Second, increasing the diffusion degree of electron cloud. The latter can be manifested by electronic spatial extent $\langle R^2 \rangle$, a term related to dispersion of electron cloud. The $\langle R^2 \rangle$ values of M^+ and M^+F^- are shown in Table S3 (Supporting Information). From Table S3, the M^+F^- species have much larger $\langle R^2 \rangle$ values compared with those of corresponding M^+ cations. Hence, the more diffuse SOMOs enable the 2s valence electron to easily escape from the M−F molecules. This fact can be confirmed by comparing the orbital energy of M^+ and M−F. From Figure 3, the repulsion from F^- anion makes the SOMO orbital energy of M^+ significantly increase and up to −2.60 ∼ −2.81 eV for the M−F species. Also, these orbital energies are higher than those of neutral M molecules (see Figure 3). Consequently, the M−F species are apt to ionize and possess low VIP values. From Table S2 (Supporting Information), the VIP values of M−F are even 0.26−0.42 eV lower than the original M molecules. Correspondingly, the LUMO orbital energy of the $(M-F)^+$ cations are as high as −3.55 ∼ −3.06 eV (at the MP2/6-311+G(3df) level), and the $(OLi_4-F)^+$, $(NLi_5-F)^+$, $(CLi_6-F)^+$, and $(BLi_7-F)^+$ cations feature low VEA values. As for Al_{14}^+, its SOMO orbital is found to vary from s to g state upon the attachment of a F^- anion (see Figure 3). Thus, the electronic configuration of Al_{14}^+ alters from $1s^21p^61d^{10}2s^21f^{14}2p^63s^1$ to $1s^21p^61d^{10}2s^21f^{14}2p^61g^1$ after fluorination; meanwhile, its SOMO orbital energy is greatly raised from −7.84 to −4.48 eV. From Table S2 (Supporting Information), the VIP value of Al_{14}−F is 0.57 eV lower compared with that of Al_{14} itself. Accordingly, the daughter cation of Al_{14}−F has a lower VEA value than that of Al_{14}^+.

Reber et al. have indicated that the same chemical principles, working for atomic clusters, can be extended to clusters with superatom motifs.[35] But is the reverse true for the present case? Specifically, do alkaline-earth fluorides have comparable low IPs with those of alkali metal atoms? Take the MgF molecule as an example. Its ionization potential is reported to be ca. 7.85 eV,[59] which is slightly higher than the IP (7.65 eV)[7] of the Mg atom. In addition, this value is much higher compared with those (3.89−5.39 eV) of alkali metal atoms. Hence, fluorination is not as effective in decreasing the ionization potential of the alkaline-earth metal atom as it is in superalkaline-earth fluoride. What makes the difference is the relative low second IP of superalkaline-earth atoms, which is attributed to the electron delocalization character of superatom motifs. In contrast, the much higher second IP (15.04 eV) of Mg atom implies that the outermost 3s electron of Mg^+ is tightly bound to the Mg nucleus. Therefore, the repulsion from F^- anion cannot rival the electron binding force of Mg^+ and produce low IP species comparable to alkali metal atoms. Accordingly, the MgF^+ cation has a higher VEA value (7.62 eV) than that (7.23 eV) of Mg^+.

To explore the dependence of the vertical electron affinity of the $(M-F)^+$ system on halogen atomic number, we also obtained the lowest energy structures of the $(OLi_4-Cl)^+$, $(OLi_4-Br)^+$, $(Al_{14}-Cl)^+$, and $(Al_{14}-Br)^+$ cations (see the Supporting Information, Figure S3). The bond energies, vertical electron affinities (VEA), and NBO charges on halogen atoms of the superalkaline-earth metal complexes $(OLi_4-X)^+$ and $(Al_{14}-X)^+$ (X = F, Cl, and Br) are listed in Table 4. As can be seen from Table 4, the bond energies of $(OLi_4-X)^+$ and $(Al_{14}-X)^+$ tend to decrease with increasing size of halogen atom X, respectively, namely 168.8 kcal/mol for $(OLi_4-F)^+$ > 131.7 kcal/mol for $(OLi_4-Cl)^+$ > 119.9 kcal/mol for $(OLi_4-Br)^+$; 136.8 kcal/mol for $(Al_{14}-F)^+$ > 98.1 kcal/mol for $(Al_{14}-$

dx.doi.org/10.1021/ja411755t | J. Am. Chem. Soc. 2014, 136, 2921−2927

Table 4. Bond Energies, E_b (in kcal/mol), Vertical Electron Affinities, VEA (in eV), and NBO Charges on Halogen Atoms (q^X) of the $(OLi_4\text{-}X)^+$ and $(Al_{14}\text{-}X)^+$ (X = F, Cl, Br) Cations

species	E_b	VEA	q^X
$(OLi_4\text{-}F)^+$	168.8	3.42	−0.856
$(OLi_4\text{-}Cl)^+$	131.7	3.60	−0.716
$(OLi_4\text{-}Br)^+$	119.9	3.65	−0.658
$(Al_{14}\text{-}F)^+$	136.8	4.87	−0.747
$(Al_{14}\text{-}Cl)^+$	98.1	4.84	−0.441
$(Al_{14}\text{-}Br)^+$	88.8	4.83	−0.336

$Cl)^+$ > 88.8 kcal/mol for $(Al_{14}\text{-}Br)^+$. This trend is consistent with the partial atomic charge on X becoming less negative, demonstrating that the M−X ionic bond strength gradually decreases with the increasing atomic number of X. It is known that the EA values of halogen atoms decrease in the order Cl > F > Br,[7] while from Table 4, the VEA values of the $(OLi_4\text{-}X)^+$ cations decrease in the order 3.65 eV (*X* = Br) > 3.60 eV (*X* = Cl) > 3.42 eV (X = F). Hence, the VEAs of $(OLi_4\text{-}X)^+$ have no direct relationship with those of involved halogen atoms. Instead, it is found that the higher electronegativity of X, the more negative charge on the X^- anion and the lower VEA of the $(OLi_4\text{-}X)^+$ cation. This confirms that the repulsive interaction between the halogen anion and valence electron cloud of OLi_4^+ is the dominant factor determining the low VIP of OLi_4−X as well as low VEA values of the $(OLi_4\text{-}X)^+$ system. In contrast, the VEAs of $(Al_{14}\text{-}Cl)^+$ and $(Al_{14}\text{-}Br)^+$ (4.84 and 4.83 eV, respectively) are quite close to that of 4.87 eV for $(Al_{14}\text{-}F)^+$. Therefore, the dependence of VEA value on halogen atomic number is not obvious for large $(Al_{14}\text{-}X)^+$ cations.

4. CONCLUSIONS

In summary, we have proposed an unusual strategy, namely halogenation, for designing cationic species with low vertical electron affinities. NBO and AIM analyses reveal that the superalkaline-earth-based fluorides $(M\text{-}F)^+$ (M = OLi_4, NLi_5, CLi_6, BLi_7, and Al_{14}) are ionic bound compounds resembling the MgF^+ cation, while the former have much larger bond energies than the latter. The investigated $(M\text{-}F)^+$ species exhibit low vertical electron affinities and represent a new kind of superalkali or pseudoalkali cations. They also possess considerable HOMO−LUMO gap values. In addition, the $(M\text{-}F)^+$ (M = OLi_4, NLi_5, CLi_6, and BLi_7) cations show high stability with respect to loss of small fragments, including the F^-, FLi_2^+, Li^+, and LiF molecules. Interestingly, the parallel study on the $(M\text{-}X)^+$ (X = F, Cl, and Br) series suggests that their VEA values are related to the electronegativity but not to the electron affinity of the involved halogen atom. What should also be noted is that halogenation has a positive effect on lowering the vertical electron affinities of superalkaline-earth cations but does not work as well for the alkaline-earth cations. In this regard, we can expect to see more superatom architectures, with desired properties, being constructed based on individual electronic characteristics of various superatom motifs, which may not be feasible in atomic dimension.

■ ASSOCIATED CONTENT

Supporting Information

Absolute energies and the Cartesian coordinates for all the optimized structures concerned, dissociation channels for the $(OLi_4\text{-}F)^+$, $(NLi_5\text{-}F)^+$, $(CLi_6\text{-}F)^+$, and $(BLi_7\text{-}F)^+$ cations, vertical ionization potentials of the M and M−F (M = OLi_4, NLi_5, CLi_6, BLi_7, and Al_{14}) molecules, optimized structures of the M, M−F (*M* = OLi_4, NLi_5, CLi_6, and BLi_7), and $(OLi_4\text{-}X)^+$, $(Al_{14}\text{-}X)^+$ (X = Cl and Br) species. This material is available free of charge via the Internet at http://pubs.acs.org.

■ AUTHOR INFORMATION

Corresponding Author

liyingedu@jlu.edu.cn

Notes

The authors declare no competing financial interest.

■ ACKNOWLEDGMENTS

This work was supported by the National Natural Science Foundation of China (Grant Nos. 21173095, 21173098, and 21303066) and the Program for New Century Excellent Talents in University of the Ministry of Education.

■ REFERENCES

(1) Khanna, S. N.; Jena, P. *Phys. Rev. Lett.* **1992**, *69*, 1664.
(2) Khanna, S. N.; Jena, P. *Phys. Rev. B* **1995**, *51*, 13705.
(3) Gutsev, G. L.; Boldyrev, A. I. *Chem. Phys.* **1981**, *56*, 277.
(4) Gutsev, G. L.; Boldyrev, A. I. *Chem. Phys. Lett.* **1982**, *92*, 262.
(5) Hotop, H.; Lineberger, W. C. *J. Phys. Chem. Ref. Data* **1985**, *14*, 731.
(6) Willis, M.; Götz, M.; Kandalam, A. K.; Ganteför, G. F.; Jena, P. *Angew. Chem., Int. Ed.* **2010**, *49*, 8966.
(7) Kerr, J. A. *CRC Handbook of Chemistry and Physics*; CRC Press: Boca Raton, 2000−2001.
(8) Wang, X.-B.; Ding, C.-F.; Wang, L.-S.; Boldyrev, A. I.; Simons, J. *J. Chem. Phys.* **1999**, *110*, 4763.
(9) Elliott, B. M.; Koyle, E.; Boldyrev, A. I.; Wang, X.-B.; Wang, L.-S. *J. Phys. Chem. A* **2005**, *109*, 11560.
(10) Wang, D.; Graham, J. D.; Buytendyk, A. M.; Bowen, K. H., Jr. *J. Chem. Phys.* **2011**, *135*, 164308.
(11) Đustebek, J.; Veličković, S. R.; Veljković, F. M.; Veljković, M. V. *Dig. J. Nanomater. Bios.* **2012**, *7*, 1365.
(12) Alexandrova, A. N.; Boldyrev, A. I.; Fu, Y.-J.; Yang, X.; Wang, X.-B.; Wang, L.-S. *J. Chem. Phys.* **2004**, *121*, 5709.
(13) Veličković, S. R.; Veljković, F. M.; Perić-Grujić, A. A.; Radak, B. B.; Veljković, M. V. *Rapid Commun. Mass Spectrom.* **2011**, *25*, 2327.
(14) Anusiewicz, I.; Sobczyk, M.; Dąbkowska, I.; Skurski, P. *Chem. Phys.* **2003**, *291*, 171.
(15) Anusiewicz, I. *J. Phys. Chem. A* **2009**, *113*, 11429.
(16) Pathak, B.; Samanta, D.; Ahuja, R.; Jena, P. *ChemPhysChem* **2011**, *12*, 2423.
(17) Gutsev, G. L.; Boldyrev, A. I. *Adv. Chem. Phys.* **1985**, *61*, 169.
(18) Rehm, E.; Boldyrev, A. I.; Schleyer, P. v. R. *Inorg. Chem.* **1992**, *31*, 4834.
(19) Alexandrova, A. N.; Boldyrev, A. I. *J. Phys. Chem. A* **2003**, *107*, 554.
(20) Sikorska, C.; Smuczyńska, S.; Skurski, P.; Anusiewicz, I. *Inorg. Chem.* **2008**, *47*, 7348.
(21) Tong, J.; Li, Y.; Wu, D.; Li, Z.-R.; Huang, X.-R. *J. Phys. Chem. A* **2011**, *115*, 2041.
(22) Tong, J.; Li, Y.; Wu, D.; Li, Z.-R.; Huang, X.-R. *J. Chem. Phys.* **2009**, *131*, 164307.
(23) Tong, J.; Li, Y.; Wu, D.; Wu, Z. J. *Inorg. Chem.* **2012**, *51*, 6081.
(24) Tong, J.; Wu, Z.; Li, Y.; Wu, D. *Dalton Trans.* **2013**, *42*, 577.
(25) Hou, N.; Li, Y.; Wu, D.; Li, Z.-R. *Chem. Phys. Lett.* **2013**, *575*, 32.
(26) Rao, B. K.; Jena, P. *J. Chem. Phys.* **1999**, *111*, 1890.
(27) Li, X.; Wu, H.-B.; Wang, X.-B.; Wang, L.-S. *Phys. Rev. Lett.* **1998**, *81*, 1909.
(28) Reveles, J. U.; Khanna, S. N.; Roach, P. J.; Castleman, A. W., Jr. *Proc. Natl. Acad. Sci. U.S.A.* **2006**, *103*, 18405.

(29) Bergeron, D. E.; Roach, P. J.; Castleman, A. W., Jr.; Jones, N. O.; Khanna, S. N. *Science* **2005**, *307*, 231.
(30) Kumar, V.; Kawazoe, Y. *Appl. Phys. Lett.* **2003**, *83*, 2677.
(31) Reveles, J. U.; Clayborne, P. A.; Reber, A. C.; Khanna, S. N.; Pradhan, K.; Sen, P.; Pederson, M. R. *Nat. Chem.* **2009**, *1*, 310.
(32) Reveles, J. U.; Sen, P.; Pradhan, K.; Roy, D. R.; Khanna, S. N. *J. Phys. Chem. C* **2010**, *114*, 10739.
(33) Medel, V. M.; Reveles, J. U.; Khanna, S. N.; Chauhan, V.; Sen, P.; Castleman, A. W., Jr. *Proc. Natl. Acad. Sci. U.S.A.* **2011**, *108*, 10062.
(34) Zhang, X.; Wang, Y.; Wang, H.; Lim, A.; Gantefoer, G.; Bowen, K. H.; Reveles, J. U.; Khanna, S. N. *J. Am. Chem. Soc.* **2013**, *135*, 4856.
(35) Reber, A. C.; Khanna, S. N.; Castleman, A. W., Jr. *J. Am. Chem. Soc.* **2007**, *129*, 10189.
(36) Wang, F.-F.; Li, Z.-R.; Wu, D.; Sun, X.-Y.; Chen, W.; Li, Y.; Sun, C.-C. *ChemPhysChem* **2006**, *7*, 1136.
(37) Li, Y.; Wu, D.; Li, Z.-R. *Inorg. Chem.* **2008**, *47*, 9773.
(38) Yang, H.; Li, Y.; Wu, D.; Li, Z.-R. *Int. J. Quantum Chem.* **2012**, *112*, 770.
(39) Wang, S.-J.; Li, Y.; Wang, Y.-F.; Wu, D.; Li, Z.-R. *Phys. Chem. Chem. Phys.* **2013**, *15*, 12903.
(40) Iwasa, T.; Nakajima, A. *J. Phys. Chem. C* **2012**, *116*, 14071.
(41) Li, Y.; Wu, D.; Li, Z.-R.; Sun, C.-C. *J. Comput. Chem.* **2007**, *28*, 1677.
(42) Schleyer, P. v. R.; Wuerthwein, E. U.; Pople, J. A. *J. Am. Chem. Soc.* **1982**, *104*, 5839.
(43) Kudo, H. *Nature* **1992**, *355*, 432.
(44) Saunders, M. *J. Comput. Chem.* **2004**, *25*, 621.
(45) Lee, C.; Yang, W.-T; Parr, R. G. *Phys. Rev. B* **1988**, *37*, 785.
(46) Reed, A. E.; Weinstock, R. B.; Weinhold, F. *J. Chem. Phys.* **1985**, *83*, 735.
(47) Carpenter, J. E.; Weinhold, F. *THEOCHEM* **1988**, *169*, 41.
(48) Cederbaum, L. S. *J. Phys. B: At. Mol. Phys.* **1975**, *8*, 290.
(49) Ortiz, J. V. *J. Chem. Phys.* **1988**, *89*, 6348.
(50) Zakrzewski, V. G.; Ortiz, J. V. *Int. J. Quantum Chem.* **1995**, *53*, 583.
(51) Boys, S. F.; Bernardi, F. *Mol. Phys.* **1970**, *19*, 553.
(52) Alkorta, I.; Elguero, J. *J. Phys. Chem. A* **1999**, *103*, 272.
(53) Frisch, M. J.; Trucks, G. W.; Schlegel, H. B.; Scuseria, G. E.; Robb, M. A.; Cheeseman, J. R.; Scalmani, G.; Barone, V.; Mennucci, B.; Petersson, G. A.; Nakatsuji, H.; Caricato, M.; Li, X.; Hratchian, H. P.; Izmaylov, A. F.; Bloino, J.; Zheng, G.; Sonnenberg, J. L.; Hada, M.; Ehara, M.; Toyota, K.; Fukuda, R.; Hasegawa, J.; Ishida, M.; Nakajima, T.; Honda, Y.; Kitao, O.; Nakai, H.; Vreven, T.; Montgomery, J. A., Jr.; Peralta, J. E.; Ogliaro, F.; Bearpark, M.; Heyd, J. J.; Brothers, E.; Kudin, K. N.; Staroverov, V. N.; Kobayashi, R.; Normand, J.; Raghavachari, K.; Rendell, A.; Burant, J. C.; Iyengar, S. S.; Tomasi, J.; Cossi, M.; Rega, N.; Millam, J. M.; Klene, M.; Knox, J. E.; Cross, J. B.; Bakken, V.; Adamo, C.; Jaramillo, J.; Gomperts, R.; Stratmann, R. E.; Yazyev, O.; Austin, A. J.; Cammi, R.; Pomelli, C.; Ochterski, J. W.; Martin, R. L.; Morokuma, K.; Zakrzewski, V. G.; Voth, G. A.; Salvador, P.; Dannenberg, J. J.; Dapprich, S.; Daniels, A. D.; Farkas, O.; Foresman, J. B.; Ortiz, J. V.; Cioslowski, J.; Fox, D. J. *GAUSSIAN 09, Revision A02*, Gaussian, Inc., Wallingford, CT, 2009.
(54) Dennington, R.; Keith, T.; Millam, J.; GaussView, Version 5, Semichem Inc., Shawnee Mission, KS, 2009.
(55) Tong, J.; Li, Y.; Wu, D.; Wu, Z.-J. *Chem. Phys. Lett.* **2013**, *575*, 27.
(56) Furuya, A.; Misaizu, F.; Ohno, K. *J. Chem. Phys.* **2006**, *125*, 094309.
(57) Bader, R. F. W. *Chem. Rev.* **1991**, *91*, 893.
(58) Han, Y.-K.; Jung, J. *J. Chem. Phys.* **2006**, *125*, 084101.
(59) Sikorska, C.; Skurski, P. *Chem. Phys. Lett.* **2010**, *500*, 211.